



HHS Public Access

Author manuscript

Nat Commun. Author manuscript; available in PMC 2014 September 03.

Published in final edited form as:

Nat Commun. ; 5: 3413. doi:10.1038/ncomms4413.

Astrocytic laminin regulates pericyte differentiation and maintains blood brain barrier integrity

Yao Yao, Zu-Lin Chen, Erin H. Norris, and Sidney Strickland

The Rockefeller University, Laboratory of Neurobiology and Genetics, 1230 York Avenue, New York, NY 10065 USA

Abstract

Blood brain barrier (BBB) breakdown is not only a consequence of, but also contributes to many neurological disorders, including stroke and Alzheimer's disease. How the basement membrane (BM) contributes to the normal functioning of the BBB remains elusive. Here we use conditional knockout mice and an acute adenovirus-mediated knockdown model to show that lack of astrocytic laminin, a brain-specific BM component, induces BBB breakdown. Using functional blocking antibody and RNAi, we further demonstrate that astrocytic laminin, by binding to integrin $\alpha 2$ receptor, prevents pericyte differentiation from the BBB-stabilizing resting stage to the BBB-disrupting contractile stage, and thus maintains the integrity of BBB. Additionally, loss of astrocytic laminin decreases aquaporin-4 (AQP4) and tight junction protein expression. Altogether, we report a critical role for astrocytic laminin in BBB regulation and pericyte differentiation. These results indicate that astrocytic laminin maintains the integrity of BBB through, at least in part, regulation of pericyte differentiation.

Introduction

The BBB is a dynamic network that regulates material exchange between circulatory system and the brain parenchyma, maintaining the homeostasis of the central nervous system (CNS)¹. BBB malfunction has been reported in many CNS disorders, including stroke, Alzheimer's disease, neuroinflammation, and various types of infections²⁻⁴. The BBB is mainly composed of brain microvascular endothelial cells, astrocytic endfeet, pericytes, and the BM⁵. Brain microvascular endothelial cells interconnect via tight junctions, forming the BBB's primary barrier^{6,7}. Astrocytes wrap around endothelial cells using their endfeet. Pericytes, sandwiched in endothelial cells and astrocytes, signal to both cell types. Recently, it has been shown that pericytes are necessary for the formation of the BBB during embryogenesis⁸ and loss of pericytes leads to compromise of BBB integrity⁹ and age-

Users may view, print, copy, and download text and data-mine the content in such documents, for the purposes of academic research, subject always to the full Conditions of use:http://www.nature.com/authors/editorial_policies/license.html#terms

Corresponding author: Sidney Strickland, Laboratory of Neurobiology and Genetics, The Rockefeller University, Box 169, 1230 York Ave, New York, NY 10065, USA, Phone: 1-212-327-8705, strickland@rockefeller.edu.

Competing financial interests

The authors declare no competing financial interests.

Contributions

Y.Y. and S.S. designed the experiments; Y.Y. carried out most experiments and data analysis; Z.C. performed the Evans blue leakage assay; Y.Y., E.N., and S.S. wrote the manuscript.

dependent vascular-mediated neurodegeneration in adult mice¹⁰, suggesting an important role of pericytes in BBB regulation.

Although damage to the BM during ischemic stroke has been linked to BBB breakdown^{11,12}, the role of the BM, especially that of individual BM components, in the BBB under physiological conditions remains elusive. The BM consists of a mixture of extracellular matrix (ECM) proteins, including laminin and collagen IV^{13–16}. Laminin is a trimeric molecule comprised of α -, β -, and γ -subunits and shows differential expression in the vascular and parenchymal BMs. Brain microvascular endothelial cells generate laminins-411 ($\alpha4\beta1\gamma1$) and -511 ($\alpha5\beta1\gamma1$)^{17,18}, whereas astrocytes produce laminins-111 ($\alpha1\beta1\gamma1$) and -211 ($\alpha2\beta1\gamma1$)^{18,19}. These laminin isoforms are all expressed by primary brain capillary pericytes²⁰. Since laminins-111 and -211 (astrocytic laminins) are only found in the vasculature of the brain, we hypothesized that astrocytic laminin might be critical for the proper functioning of the BBB. Given the critical regulatory role of astrocytic laminin in vascular smooth muscle cells²¹, we further hypothesize that astrocytic laminin may regulate the differentiation of pericytes, cells that belong to the same lineage as vascular smooth muscle cells.

Here we show that lack of astrocytic laminin induces pericyte differentiation from the resting stage to the contractile stage, switching pericyte function from stabilizing the BBB to compromising it. Additionally, lack of astrocytic laminin also abrogates the polarity of astrocytic endfeet and the expression of tight junction proteins in endothelial cells. These results support an important role of astrocytic laminin in the maintenance of BBB integrity.

Results

Genetic ablation of glial laminin induces BBB breakdown

To investigate the role of astrocytic laminin on BBB integrity, we generated conditional laminin knockout mice ($N\gamma1$ -KO) by crossing homozygous floxed laminin $\gamma1$ (F/F) mice with Nestin-Cre transgenic mice. Since nestin is expressed by neural progenitor cells, which give rise to neurons and glia, laminin should be deficient in both neurons and glia in the $N\gamma1$ -KO mice, which we have validated²¹. To investigate when laminin expression was abrogated, we examined laminin $\gamma1$ expression by immunohistochemistry at different stages. At embryonic day 15.5 (E15.5), laminin $\gamma1$ level was unaffected in $N\gamma1$ -KO brain compared to their littermate controls (Ctr) (Supplementary Fig. 1). At E18.5 and postnatal day 2 (P2), on the other hand, a dramatic decrease of laminin $\gamma1$ was observed in $N\gamma1$ -KO brain (Supplementary Fig. 1), suggesting that laminin expression was disrupted at late embryonic stages in $N\gamma1$ -KO mice. Although brain capillary pericytes have been reported to express nestin²², we did not observe nestin and PDGFR β double positive cells in the striatum of the $N\gamma1$ -KO mice (Supplementary Fig. 2a). This nestin antibody specifically labeled neural stem cells in the subgranular zone (Supplementary Fig. 2b), suggesting that PDGFR β positive pericytes do not express nestin. In addition, EGFP was expressed in brain parenchymal cells (neurons and astrocytes) (Supplementary Fig. 3b) but absent in PDGFR β ⁺ pericytes in ROSA26-EGFP^{+/+} Nestin-Cre^{+/+} mice (Supplementary Fig. 3a). In Ctr (ROSA26-EGFP^{+/+} Nestin-Cre^{-/-}) mice, EGFP was totally absent due to the lack of Cre expression (Supplementary Fig. 3). These data suggest that Cre is not expressed in pericytes

in the N γ 1-KO mice. To further investigate whether pericytic laminin is affected in this N γ 1-KO mouse line, we isolated primary pericytes from Ctr and mutant brain microvessels and examined their laminin γ 1 expression. The purified pericytes were positive for PDGFR β and CD13 (pericyte markers), while negative for CD31 (Supplementary Fig. 4a–d), indicative of high purity. The specificity of the CD31 antibody was validated in purified primary brain capillary endothelial cells (Supplementary Fig. 4e–f). *Laminin γ 1* mRNA was detected in pericytes from both Ctr and N γ 1-KO mice (Supplementary Fig. 5a), and qRT-PCR showed that *laminin γ 1* mRNA levels in the pericytes from N γ 1-KO mice was comparable to that from Ctr mice (Supplementary Fig. 5b). Consistently, we detected laminin γ 1 protein expression in primary pericytes from the N γ 1-KO mice (Supplementary Fig. 4c and d), suggesting that pericytic laminin is not affected in the N γ 1-KO mice. We further examined laminin expression in pericytes *in vivo* using anti-laminin α 2 antibody as lack of laminin γ 1 leads to intracellular degradation of α and β chains²³ and found that laminin α 2 co-localized with CD13 and PDGFR β in both Ctr and N γ 1-KO mice (Supplementary Fig. 6), although laminin α 2 expression level was lower in N γ 1-KO mice. Since laminin α 2 is not expressed in endothelial cells, and N γ 1-KO mice²¹ and laminin γ 1 knockdown mice (see Fig. 4c) have a deficiency of laminin α 2 expression in astrocytes, our results suggest that laminin α 2 expression is from pericytes in the N γ 1-KO mice. The lower expression level of laminin α 2 in the N γ 1-KO mice is due to the absence of laminin α 2 in astrocytes. Altogether, our data suggest that the N γ 1-KO mouse line does not knockout laminin in pericytes.

Next, we injected Evans blue intraperitoneally and found leakage of this dye into the brain parenchyma of N γ 1-KO mice but not in Ctr mice (Fig. 1a). Consistent with this result, we detected mouse IgG in the brain parenchyma of N γ 1-KO mice but not that of Ctr mice (Fig. 1b and c). In a quantitative study, we found more intravenously injected FITC-Dextran (500kD) in homogenates of N γ 1-KO brains than in those of Ctr brains (Fig. 1d). These data indicate that BBB integrity is compromised in N γ 1-KO mice. To determine if neuronal or glial laminin is responsible for the BBB breakdown phenotype in the N γ 1-KO mice, we also generated conditional neuronal laminin knockout mice, termed C γ 1-KO, by crossing F/F mice with CamKII-Cre transgenic mice. The C γ 1-KO mice showed no signs of BBB disruption²⁴ (Fig. 1a–c), suggesting that the BBB breakdown phenotype in the N γ 1-KO mice is due to the lack of laminin in glial cells, not neurons.

Changes in individual BBB components in N γ 1-KO mice

Astrocytes express AQP4 exclusively at their endfeet to regulate water homeostasis at the vessel-neuron interface²⁵. In Ctr mice, we found high level of AQP4, which co-localized with endothelial cell marker CD31 in capillaries (Fig. 2a), indicating that these astrocytic endfeet were polarized. In N γ 1-KO mice, however, AQP4 expression was dramatically decreased at astrocytic endfeet in capillaries (Fig. 2a). Consistently, Western blots showed a significant decrease of AQP4 expression in the striatum of N γ 1-KO mice (Fig. 2c), suggesting that the polarity and possibly function of the astrocytic endfeet are lost in N γ 1-KO mouse brains.

Brain microvascular endothelial cells form the primary barrier of the BBB by connecting to each other via tight junctions, where tight junction proteins are expressed^{26,27}. Although blood vessel density was not affected, as determined by immunostaining for CD31 (Fig. 2a), the levels of occludin and claudin-5, two major protein components of tight junctions, were significantly decreased in the capillaries of N γ 1-KO mice (Fig. 2b). Consistently, Western blots showed diminished expression of occludin and claudin-5 in the striatum of N γ 1-KO mice (Fig. 2c), suggesting compromise of the tight junction structure in N γ 1-KO mice.

In addition to capillaries, we also examined how loss of astrocytic laminin affected the expression of AQP4 and tight junction proteins in large blood vessels. No decrease of AQP4, occludin and claudin-5 was observed in large vessels in N γ 1-KO mice (Supplementary Fig. 7). Quantitative western blots using large blood vessels showed that claudin-5 was significantly increased in N γ 1-KO mice (Supplementary Fig. 7). These data suggest that loss of astrocytic laminin predominantly affects capillaries in the brain, and defects in capillaries, rather than big blood vessels, are responsible for the BBB leakage phenotype in N γ 1-KO mice.

Sandwiched between astrocytes and endothelial cells in capillaries, pericytes also contribute to the integrity of the BBB⁸⁻¹⁰. We examined the expression of PDGFR β , a pericyte marker, and found no obvious difference between Ctr and N γ 1-KO brains (Fig. 2b). Consistent with this result, Western blot results did not show a difference in PDGFR β expression in the striatum of Ctr and N γ 1-KO mice (Fig. 2c).

To study the ultrastructure of BBB components, we examined brain samples from Ctr and N γ 1-KO mice using electron microscopy (EM). In Ctr mice, pericytes were sandwiched in between well-organized astrocytes and endothelia. The BM between astrocytes and pericytes (blue arrows) and that between pericytes and endothelial cells (green arrowheads) were compact (Fig. 3a). In N γ 1-KO mice, however, pericytes changed their morphology (Fig. 3a), indicating that pericyte differentiation and/or maturation may be affected. In addition, in N γ 1-KO mice, both BMs were patchy and diffuse (red arrows, Fig. 3a) and endothelial membrane integrity was compromised (white stars, Fig. 3a), suggesting that glial laminin may regulate pericyte differentiation and maturation.

Lack of astrocytic laminin leads to BBB breakdown

Glia includes astrocytes and oligodendrocytes. Astrocytic endfeet wrap around endothelial cells and pericytes, while oligodendrocytes do not participate in the formation of BBB directly. Therefore, we hypothesized that it is the lack of astrocytic laminin that induces BBB disruption. To test this hypothesis, we acutely knocked down the expression of laminin specifically in astrocytes by injecting adenovirus expressing Cre under a GFAP promoter (Ad-pGFAP-Cre, kindly provided by Dr. Alvarez-Buylla) into adult F/F mice. Wild-type (C57Bl6) mice injected with Ad-pGFAP-Cre and F/F mice injected with adenovirus expressing GFP only (Ad-GFP) were used as Ctrs. To examine the cell types expressing Cre after Ad-pGFAP-Cre injection, we performed immunohistochemistry on brains collected seven days after injection. We found that Cre co-localized with the astrocyte marker GFAP, but not the neuronal marker TUJ1 or pericyte marker PDGFR β (Supplementary Fig. 8), indicating Cre is specifically expressed in astrocytes after injection. Leakage of Evans blue

and mouse IgG was observed in F/F mice seven days after Ad-pGFAP-Cre injection, but not in Ctrs (Fig. 4a). We further noticed that extravasated IgG co-localized well with Cre in F/F mice injected with Ad-pGFAP-Cre (Fig. 4a). The quantification of IgG intensity showed a significant increase in Cre positive area in F/F mice injected with Ad-pGFAP-Cre, but not the Ctrs (Fig. 4b). GFP (for F/F+Ad-GFP) and Cre (for C57+Ad-pGFAP-Cre and F/F+Ad-pGFAP-Cre) immunohistochemistry revealed similar size of infected areas (Fig. 4a), suggesting that BBB breakdown in Ad-pGFAP-Cre injected F/F mice was not due to different virus titer/dose. These data suggest that acute ablation of astrocytic laminin alone is sufficient to induce BBB breakdown.

To validate that the disruption of BBB integrity was actually due to the lack of astrocytic laminin, we examined the expression of laminin in these mice. Given the differential expression of laminin isoforms in the neurovascular unit, laminin $\alpha 2$ and $\alpha 4$ were used as markers for astrocytic and endothelial laminin, respectively. Wild-type mice with Ad-pGFAP-Cre injection and F/F mice with Ad-GFP injection did not show any changes in the expression of laminins $\alpha 2$ and $\alpha 4$ (Fig. 4c and d). Injection of Ad-pGFAP-Cre into F/F mice, however, decreased the expression of laminin $\alpha 2$ without affecting laminin $\alpha 4$ expression (Fig. 4c and d), indicating specific knockdown of laminin in astrocytes. In addition, we also examined TUNEL staining seven, thirty and sixty days after adenovirus injection. No TUNEL positive cells were found at the injection site (Supplementary Fig. 9), whereas recombinant DNase I pretreated brain sections showed a large number of TUNEL⁺ cells (positive control). These results suggest that the conditions we used did not cause apoptotic cell death, and that astrocytic laminin is necessary for the maintenance of BBB integrity.

Lack of astrocytic laminin affects BBB components

We next investigated how lack of astrocytic laminin affects individual components of the BBB. Like N γ 1-KO mice, APQ4 expression was dramatically decreased in F/F mice injected with Ad-pGFAP-Cre, but not in the Ctrs (Fig. 5a). The expression levels of occludin (Fig. 5b) and claudin-5 (Fig. 5c) followed the same trend.

Interestingly, F/F mice with Ad-pGFAP-Cre injection showed up-regulation of PDGFR β compared to the Ctrs (Fig. 5d), suggesting that astrocytic laminin may affect the proliferation or differentiation of pericytes. To investigate this further, we examined the expression of Ki67, a proliferation marker. Neither total Ki67⁺ nor Ki67⁺ PDGFR β ⁺ cell numbers in Ad-pGFAP-Cre injected F/F mice showed a difference compared to the Ctrs (Supplementary Fig. 10), suggesting that differentiation, rather than proliferation, is responsible for the enhanced expression of PDGFR β in the acute astrocytic laminin knockdown model.

We also performed EM analysis using brain samples from these adenovirus-injected mice (Fig. 3b). In the Ctrs, astrocytes, pericytes, and endothelial cells were well-organized. Pericytes were surrounded by BMs secreted by endothelial cells (green arrowheads) and astrocytes (blue arrows) (Fig. 3b). In astrocytic laminin-knockdown mice (F/F+Ad-pGFAP-Cre), however, morphological change was observed in capillary pericytes (Fig. 3b). Similar to N γ 1-KO mice, these astrocytic laminin-knockdown mice showed patchy and diffuse BMs

(red arrows, Fig. 3b) and the BMs were difficult to define at some places (white stars, Fig. 3b). Additionally, pericyte and endothelial membrane integrity was disrupted and unclear at certain locations in these mice (Fig. 3b). Altogether, our data suggest that astrocytic laminin regulates pericyte differentiation and maturation.

Laminin-111 blockage promotes pericyte differentiation

Pericytes are multipotent stem and/or progenitor cells, which can be differentiated into many different cell types *in vitro*^{28,29}. Although markers for pericytes at different differentiation stages are not well defined, smooth muscle actin- α (SMA) is used as a marker of differentiation³⁰ and SMA^{high} pericytes are more often found in abnormal conditions²⁸, including fibrotic tissue and tumors. It has been shown that only a small portion of pericytes are positive for SMA in the brain *in vivo*^{29,31}. In primary cultures, less than 5% of freshly isolated brain capillary pericytes express SMA^{14,32}, but all of them become SMA positive by day 7^{33–35}. These results suggest that components from the brain, such as the astrocytic BM, a brain-specific protein mixture that has direct contact with pericytes, may regulate the expression of SMA in pericytes³⁶ and hence pericyte differentiation. Together with our EM results and *in vivo* data, we further hypothesized that astrocytic laminin inhibits SMA expression in pericytes, thereby preventing pericyte differentiation. To test this hypothesis, we plated primary pericytes on laminin-111 (astrocytic laminin)-coated plates and treated them with laminin-111 blocking antibody or Ctr IgG. Consistent with our *in vivo* data, laminin-111 blockage induced an up-regulation of PDGFR β (Fig. 6a). SMA and another contractile protein---SM22-alpha (SM22- α) were also increased after laminin-111 blockage (Fig. 6a), suggesting that laminin-111 maintains pericytes in an undifferentiated or less differentiated stage with low levels of contractile proteins.

Although pericytes and vascular smooth muscle cells belong to the same lineage and category²⁸, they respond differently to laminin. It has been shown that laminin promotes the expression of contractile proteins in vascular smooth muscle cells^{37,38} and this effect is mediated by transcriptional factor myocardin^{39,40}. To investigate whether the same signaling pathway is activated in pericytes, we examined myocardin levels in pericytes after laminin-111 blocking antibody treatment. Myocardin level was not affected by laminin-111 blockage (Fig. 6a), suggesting that pericytes and vascular smooth muscle cells use different mechanisms to regulate contractile protein expression.

Additionally, pericytes were treated with conditioned medium from astrocytes, and the expression of PDGFR β , SMA, SM22- α , and myocardin was examined by Western blot. As expected, none of these markers was affected (Supplementary Fig. 11), suggesting that the increased expression of PDGFR β and contractile proteins is not due to soluble factors secreted by astrocytes.

To exclude the possibility that pericyte-secreted laminin-411 also contributes to the enhanced expression of PDGFR β and contractile proteins, we applied laminin α 4-specific blocking antibody to cultures. Blockage of laminin α 4 did not affect any of the proteins examined (Fig. 6b), suggesting that it is astrocytic laminin that regulates the differentiation of pericytes.

Laminin regulates pericyte differentiation via integrin $\alpha 2$

To identify the receptor(s) that mediates astrocytic laminin-induced pericyte differentiation, we treated primary pericytes plated in laminin-111 coated plates with functional blocking antibodies to integrin $\alpha 2$ (ITGA2) and integrin $\beta 1$ (ITGB1). ITGA2 blockage significantly enhanced the expression of PDGFR β , SMA, and SM-22 α while ITGB1 blockage did not affect the expression of these markers (Fig. 7a), suggesting that ITGA2 but not ITGB1 is involved in astrocytic laminin-induced pericyte differentiation. The expression of myocardin, as expected, was not affected by these blocking antibodies (Fig. 7a), again suggesting that pericytes and vascular smooth muscle cells have different regulatory machinery in contractile protein expression.

To confirm the role of ITGA2 in pericyte differentiation, we genetically ablated ITGA2 expression using a shRNA-mediated knockdown technique. Three shRNA sequences targeting ITGA2 (Lenti-shRNA-1-3) and one scramble sequence (Lenti-shRNA-scramble; Ctr) were used (Fig. 7b). Seven days after transduction, we detected a significant decrease of ITGA2 expression by Western blot, where Lenti-shRNA-1 was the most efficient (Fig. 7c). Next, we transduced pericytes with Lenti-shRNA-1 and Lenti-shRNA-scramble for 7 days and found that Lenti-shRNA-3 significantly increased the expression of PDGFR β , SMA, and SM-22 α , without affecting myocardin level (Fig. 7d). These data suggest that ITGA2 is indeed the receptor that mediates astrocytic laminin-induced pericyte differentiation and myocardin does not regulate contractile protein expression in pericytes.

Astrocytic laminin regulates pericyte differentiation *in vivo*

To investigate whether astrocytic laminin regulates pericyte differentiation *in vivo*, we first examined SMA expression in PDGFR β positive pericytes in Ctr and N $\gamma 1$ -KO mice. In Ctr brains, no SMA expression was found in PDGFR β positive pericytes (Fig. 8a). In N $\gamma 1$ -KO mice, however, SMA and PDGFR β double positive pericytes were observed in the deep brain regions, such as striatum, basal ganglia, thalamus and hypothalamus, but not in the cortex or hippocampus (Fig. 8a). The quantification of SMA intensity normalized by PDGFR β intensity revealed a significant difference between Ctr and N $\gamma 1$ -KO mice in the deep brain regions, but not in cortex or hippocampus (Fig. 8a). Next, we examined SMA expression in capillary pericytes in the acute model. GFP and Cre immunohistochemistry was used to locate the infection site. Ad-pGFAP-Cre injection in F/F mice induced SMA expression in PDGFR β positive capillary pericytes, whereas pericytes from Ctr animals were SMA negative (Fig. 8b). Quantification showed a significant increase of SMA expression in capillary pericytes in Cre positive region (Fig. 8b). Altogether, our data suggest that lack of astrocytic laminin induces differentiation of capillary pericytes *in vivo*.

The phenotypes observed in N $\gamma 1$ -KO mice are brain-specific

To investigate whether the capillary leakage and pericyte differentiation phenotypes in N $\gamma 1$ -KO mice are unique to the brain, we also performed permeability and pericyte differentiation assays in peripheral organs, including liver, kidney and spleen. The levels of IgG in liver, kidney, and spleen were similar between Ctr and N $\gamma 1$ -KO mice (Supplementary Fig. 12a), suggesting that capillary permeability was not affected in the peripheral system in N $\gamma 1$ -KO mice. Next, we further examined SMA expression in PDGFR β positive pericytes

and found no difference between Ctr and N γ 1-KO mice in these organs (Supplementary Fig. 12b), suggesting that pericyte differentiation was not modified in the peripheral system in N γ 1-KO mice. Altogether, our data indicate that the phenotypes we observed in N γ 1-KO mice are brain-specific, probably due to the exclusive distribution of astrocytes in the brain.

Discussion

In as early as 1963, researchers noticed that emigrating leukocytes are more often found between the endothelium and BM than in the progress of passing between endothelial cells⁴¹, suggesting that the BM acts as a distinct barrier of the BBB and offers resistance to migrating leukocytes^{41,42}. However, the normal physiological roles of the BM and its components in BBB regulation remain elusive, probably due to the complexity of BM composition and the lack of animal models and research tools. Using conditional laminin γ 1 knockout mice and an adenovirus-mediated astrocyte-specific laminin knockdown technique, we report that lack of astrocytic laminin leads to breakdown of the BBB. Further mechanistic studies showed that lack of astrocytic laminin affected astrocytic endfeet polarity, pericyte differentiation, and endothelial tight junction protein expression. This is, to our knowledge, the first study reporting a crucial role of astrocytic laminin on the maintenance of BBB integrity in physiological condition. Our studies also for the first time, to our knowledge, reveal that laminin-111 actively regulates the differentiation of pericytes.

Our data show that BBB breakdown and pericyte differentiation are predominantly found in deep brain regions, including striatum, basal ganglia, thalamus and hypothalamus, and rarely found in cortex and hippocampus in the N γ 1-KO mice. The exact mechanism responsible for this regional difference is not clear. However, pia matter may be one possible explanation. Pia matter synthesizes laminin-111 and 211 (astrocytic laminin) and covers blood vessels in surface regions, including cortex^{43,44}. In the surface brain regions of N γ 1-KO mice, the loss of astrocytic laminin could be compensated by laminin from pia matter. In deep brain regions, however, this compensation mechanism does not exist due to the lack of pia matter, leading to BBB breakdown and pericyte differentiation. Another possibility is that the astrocyte heterogeneity may contribute to the regional difference. Astrocytes from different brain regions have different morphology, gene expression profiles and biological functions^{45,46}. It is possible that the unique properties of astrocytes in deep brain regions (anatomical structure, gene expression profiles, relationship to pericytes, function) are responsible for the regional difference.

Astrocytes, the most abundant cell type in the brain, wrap around endothelial cells and pericytes with their polarized endfeet, participating in the formation of the BBB. AQP4, a water channel protein exclusively expressed on astrocytic endfeet that regulates water homeostasis at the vessel-neuron interface²⁵, has been shown to play an important role in BBB regulation^{9,47,48}. Mice deficient in pericytes lack an astrocytic BM, have a leaky BBB, and lose AQP4 expression in astrocytic endfeet⁹. BBB compromise has also been reported in the dystrophin-deficient mdx mice, which have age-dependent reduction of AQP4 expression in astrocytes^{47,48}. In addition, patchy distribution of AQP4 and other astrocyte endfeet proteins is also reported in mice lacking astrocytic integrin β 1, a major receptor for astrocytic laminin⁴⁹. Consistent with these reports, we found decrease of AQP4 and BBB

breakdown in mice lacking astrocytic laminin, indicating a pivotal role of astrocytic laminin in the regulation of astrocytic polarity and BBB function.

Recently, pericytes have been shown to play an important role in the regulation of vascular permeability^{9,10} and formation of the BBB⁸. Acute ablation of laminin expression by adenoviral injection compromised BBB integrity, up-regulated expression of the pericyte marker PDGFR β , but did not affect pericyte proliferation, linking laminin to pericyte differentiation. Although many cellular markers, including SMA, PDGFR β , and CD13 have been suggested for pericytes^{28,50}, the expression of these markers is highly dynamic depending on the developmental stage and pathological conditions²⁸. Additionally, other cells also share these markers with pericytes²⁸. We showed *in vitro* that blockage of laminin-111 converted pericytes from a stage with low levels of SMA, SM22- α , and PDGFR β , to one with high levels of these proteins, suggesting that pericytes have at least two differentiation stages (contractile protein^{low} and ^{high}) and that laminin-111 inhibits their differentiation to the contractile protein^{high} stage. Furthermore, we observed that SMA was expressed in capillary pericytes in deep brain regions of N γ 1-KO and Ad-pGFAP-Cre injected F/F mice but not Ctr brains, suggesting that astrocytic laminin is inhibitory to pericyte differentiation *in vivo* and that the differentiated SMA^{high} pericytes destabilize BBB integrity. These results are consistent with the report that TGF β -treated pericytes, which express high levels of SMA, decreased BBB integrity; whereas bFGF-treated pericytes, which express low levels of SMA, stabilize the barrier integrity³⁰. Goritz and colleagues classified pericytes into two subclasses: type A (SMA⁻, Glast⁺, Desmin⁻, PDGFR β ⁺) and type B (SMA⁺, Glast⁻, Desmin⁺, PDGFR β ⁺)⁵¹. They reported that SMA⁻ type A pericytes left blood vessel wall and became SMA⁺ in a spinal cord injury model⁵¹, again suggesting that SMA⁺ pericytes destabilize BBB integrity. Taken together, we propose a model showing how astrocytic laminin affects pericyte differentiation and BBB integrity (Fig. 9). Pericytes embedded in BMs express low levels of PDGFR β and contractile proteins (SMA and SM22- α), defined as resting stage. Upon injuries that cause loss of BM, especially laminin-111, pericytes change their morphology and switch to a stage with high levels of contractile proteins and PDGFR β , defined as the contractile stage. The differentiation from the resting stage to the contractile stage changes the functions of pericytes from barrier stabilization to barrier disruption. Furthermore, our data suggest that this functional conversion is mediated by ITGA2.

Unlike pericytes, which cover capillaries²⁸, vascular smooth muscle cells are found in arteries and arterioles. Vascular smooth muscle cells can switch between two phenotypes: a synthetic phenotype and a contractile phenotype⁵². We and others have shown that laminin induces SMA expression in vascular smooth muscle cells^{21,37,38}, promoting a contractile phenotype. Altogether, these data suggest a different role of laminin on pericytes and vascular smooth muscle cells - laminin promotes the differentiation of vascular smooth muscle cells to the contractile phenotype, but maintains pericytes in their resting stage. These results can be explained given the location and function of these cells. Vascular smooth muscle cells regulate arterial blood pressure and local blood flow⁵². Thus, the contractile phenotype should be maintained under physiological conditions. Pericytes actively regulate BBB integrity^{8-10,28}, although they may also constrict capillaries under

pathological conditions^{53–55}. Given that the size of a capillary is less than 8 μm ⁵⁶, which allows the passage of only one red blood cell at a time, it is logical for pericytes to have a resting state under physiological conditions to allow patency of the vessel. The next question then becomes: how does laminin exert different roles in pericytes and vascular smooth muscle cells? Our data show that ITGA2 actively regulates pericyte differentiation, but it is not expressed in vascular smooth muscle cells (Supplemental Fig. 13). Additionally, myocardin, a transcriptional factor known to regulate vascular smooth muscle differentiation, is not affected by laminin-111 blockage or ITGA2 blockage/knockdown in pericytes, suggesting that pericytes and vascular smooth muscle cells use different molecular mechanisms to regulate their differentiation.

Our results showed that PDGFR β levels were dramatically increased in the adenoviral injection experiments, but not affected in N γ 1-KO brains. This discrepancy could be due to compensatory mechanisms. Adenoviral injection in adult mice knocks down the expression of laminin γ 1 acutely, while long-term loss of laminin γ 1 is found in the N γ 1-KO mice. The long-term loss of laminin γ 1 may activate compensatory mechanisms, which act to decrease PDGFR β levels. In the acute model, on the contrary, these mechanisms may not yet be activated. Similar compensation was reported previously^{57–59}. No abnormalities of neural stem cell behavior were reported in integrin α 6^{-/-} mice⁵⁹ or mice lacking ITGB1 specifically in these cells⁵⁸. Transient ablation of ITGB1 in embryonic brains by blocking antibody, however, resulted in abnormal neural stem cell proliferation, dystrophic radial glia fibers, and substantial layering defects in the postnatal neocortex⁵⁷.

In summary, we report a critical role of astrocytic laminin in the maintenance of BBB integrity under normal conditions. Astrocytic laminin polarizes astrocytic endfeet, inhibits pericyte differentiation, and induces/maintains tight junction protein expression in endothelial cells. Our data provide novel molecular targets to manipulate BBB integrity and thus promote the development of effective drugs or therapeutic reagents for many CNS diseases.

Methods

Animals

Wild-type (C57BL/6), homozygous floxed laminin γ 1 (F/F) mice, Nestin-Cre, CaMKII-Cre, GFAP-Cre, and ROSA26-EGFP transgenic mice were maintained in the Comparative Biosciences Center at The Rockefeller University with free access to water and food. F/F mice were crossed with these transgenic mouse lines to generate conditional laminin knockout mice (laminin expression was not successfully decreased in astrocytes in F/F GFAP-Cre mice). Two-four-month-old knockout mice (both genders) and age-matched controls (both genders) were used to perform experiments. Experimental procedures were in accordance with the NIH guide for care and use of animals and approved by the Animal Care and Use Committee at The Rockefeller University.

Cell Culture and Treatments

Primary human brain vascular pericytes, vascular smooth muscle cells, and astrocytes were purchased from ScienCell and maintained in their respective media (ScienCell) and/or DMEM supplemented with 10% FBS. When cells reached 70% confluence, dialyzed anti-laminin-111 blocking antibody (Sigma, L9393, 25 µg per ml), anti-laminin α4 blocking antibody 2A3 (kindly provided by Dr. Jonathan Jones, non-diluted), anti-ITGA2 blocking antibody (Millipore, MAB1950Z, 25 µg per ml), anti-ITGB1 blocking antibody (BD, 555002, 25 µg per ml), or anti-rabbit IgG (Sigma, R5506, 25 µg per ml) were added to the media. Media was replaced every 2 days. On day 7, cells were collected and lysed with RIPA buffer (50mM Tris, pH 7.4, 1% NP-40, 0.5% Na-deoxycholate, 1% SDS, 150 mM NaCl, 2 mM EDTA, 1X protease inhibitor cocktail, and 1X phosphatase inhibitor cocktail).

Primary brain pericytes were isolated and cultured as described^{22,60}. Briefly, brains from 2–4 month-old Ctr and Nγ1-KO mice (both males and females) were collected under aseptic conditions, followed by homogenization in DMEM + 5% FBS. After centrifugation, the pellet was resuspended in 17% dextran solution and centrifuged at 6000 g for 15 minutes at 4. Blood vessels were collected at the bottom and resuspended in DMEM + 5% FBS. These vessels were sequentially filtered through 100 µm and 40 µm cell strainers. Microvessels trapped by 40 µm cell strainer were collected and digested with 1 mg per ml collagenase/dispase (Roche) for 4 hours at 37. After digestion, the vessels were triturated with pipette and plated in uncoated plastic plates. After 8 hours, unattached cells were removed by shaking and gentle pipetting. The attached pericytes were then grown in pericyte medium (ScienCell).

Large Blood Vessel Isolation

Large blood vessels were isolated as previous described with minor modifications^{22,60,61}. Briefly, brains from Ctr and Nγ1-KO mice were collected, homogenized and centrifuged in dextran solution as described above. Blood vessel pellet was then filtered through 100 µm cell strainers. Large blood vessels trapped by the strainer were collected and homogenized in tissue lysis buffer (100mM Tris, pH 8, 1% SDS, 200 mM NaCl, 5 mM EDTA, 1X protease inhibitor cocktail, 1X phosphatase inhibitor cocktail).

PCR and qRT-PCR

Total RNA was extracted from primary pericytes using Trizol (Invitrogen), according to manufacturer's instructions. The RNA was further purified by RNeasy Kit (Invitrogen). Equal amount of total RNA was subjected to reverse transcription using the SuperScript III First-Strand Synthesis System (Invitrogen) as instructed. For PCR, the following primers were used. *Laminin γ1*: 5'-TGGGCAGAATCTTTCCTTCT-3', 5'-ACAGAACTGTCCCCCGTATC-3'; *Actin*: 5'-ACAGCTGAGAGGGAAATCGT-3', 5'-TGCTAGGAGCCAGAGCAGTA-3'. For qRT-PCR, *laminin γ1* and *GAPDH* ready-to-use gene expression assays (Invitrogen), master-mix (Applied Biosystems), and cNDA were mixed together and the reaction was run in ABI HT7900 Fast Real-Time PCR System. The expression level of *laminin γ1* was normalized to housekeeping gene *GAPDH*.

Lentivirus Generation

Lentiviruses were purchased from GenTarget. Three shRNA sequences against human ITGA2 (1: AAGGAAGAGTCTACCTGTTTACGAGTAAACAGGTAGACTCTTCCTT, 2: GGTGACCAGATTGGCTCCTATCGAGATAGGAGCCAATCTGGTCACC, 3: CTGGAGTGGCTTTCCTGAGAACGAGTTCTCAGGAAAGCCACTCCAG) and one scrambled sequence (GTCTCCACGCGCAGTACATTTTCGAGAAATGTACTGCGCGTGGAGAC) were cloned into GenTarget's lentiviral shRNA expression vector with RFP-puromycin marker. Sequence-verified lentivectors and lentiviral packaging plasmids were co-transfected into lentivirus production cell lines. The packaged lentiviruses were collected from the medium and filtered through 0.45µm filter.

ITGA2 knockdown

Pericytes were plated in laminin-111 coated plates. When cells reached 50% confluence, 8 µg per ml polybrene and the appropriate amount of lentivirus were added to reach a final MOI of 2 (2 lentiviruses per cell). Medium was replaced 96 hours after transduction. Pericyte lysates were collected 7 days after transduction.

Striatum Dissection

Ctr and N γ 1-KO mice were anesthetized with avertin (0.02 ml per g of body weight) intraperitoneally. After perfusion with saline, brains were collected and placed under a dissection microscope. Cortices and hippocampi were carefully removed, and the striatum was homogenized in tissue lysis buffer.

Western Blot

Total protein concentration from the lysates was determined using the Bio-Rad protein assay kit. Equal amount of protein was loaded and separated in 10% or 12% SDS-PAGE, followed by transfer to PVDF membrane (Millipore). The membranes were then incubated with anti-AQP4 (Millipore, AB3594, 1:500), anti-occludin (Invitrogen, 71-1500, 1:1000), anti-ZO-1 (Invitrogen, 40-2200, 1:1000), anti-Claudin-5 (Invitrogen, 34-1600, 1:1000), anti-PDGFR β (Cell Signaling, 3169S, 1:500), anti-SMA (Sigma, F3777, 1:1000), anti-SM22- α (GeneTex, GTX113561, 1:1000), anti-integrin α 2 (Millipore, AB1936, 1:500), anti-myocardin (R&D, MAB4028, 1:500) and anti-actin (Sigma, A5441, 1:2000) antibodies at 4 overnight, followed by incubation with HRP-conjugated secondary antibodies (Jackson ImmunoResearch Lab). The proteins were visualized by SuperSignal West Pico Chemiluminescent Substrate (Pierce). The density of bands was normalized to actin and quantified using NIH Image J.

Stereotaxic Injection

Ad-GFP (SignaGen) and Ad-pGFAP-Cre (kindly provided by Dr. Arturo Alvarez-Buylla) were propagated and purified twice by cesium chloride banding, followed by dialysis in phosphate buffered saline. 3×10^8 plaque-forming units of these adenoviruses were used for injection. Wild-type or F/F mice (2–3 months, 25–35 g, both genders) were anesthetized as described above. After making an incision, a burr hole was drilled at stereotaxic coordinates

of -1 mm posterior to bregma and 2.5 mm lateral from midline. Then, adenoviruses were injected into the brain at the depth of 3.5 mm over 5 minutes. The needle was kept in place for 2 minutes to prevent reflux. Seven days after injection, the mice were transcardially perfused and the brains were sectioned.

BBB Permeability Assays

Twelve hours before the mice were sacrificed, 2% Evans blue in saline was injected into Ctr, N γ 1-KO and C γ 1-KO mice intraperitoneally at the concentration of 10 μ l per g body weight. After perfusion with saline, the brains were collected and sectioned. BBB breakdown was revealed by visualizing Evans blue at 620 nm under the fluorescence microscope. Mouse IgG was co-immunostained with CD31 and visualized at 555 nm. The quantification of IgG leakage was performed as described previously with minor modifications⁶². Briefly, IgG fluorescent intensity at specific brain regions was determined using ImageJ software. The mean fluorescent intensity per pixel was quantified by using at least 9 random images from at least 3 animals. In addition, 100 μ l FITC-Dextran (500 kD, 10 mg per ml) was injected into 2-3 month-old Ctr, N γ 1-KO and C γ 1-KO mice intravenously. After perfusion, brain lysates were collected and the leakage of this dye into the brain was examined using a fluorescence plate reader at 488 nm.

Immunohistochemistry

Brain sections were immunostained with anti-laminin γ 1 (Abcam, AB3297, 1:200), anti-laminin-111 (Sigma, L9393, 1:1000), anti-laminin α 2 (Sigma, L0663, 1:200), anti-laminin α 4 (R&D system, AF3837, 1:200), anti-AQP4 (Millipore, AB3594, 1:500), anti-occludin (Invitrogen, 71-1500, 1:500), anti-ZO-1 (Invitrogen, 40-2200, 1:500), anti-Claudin-5 (Invitrogen, 34-1600, 1:500), anti-CD31 (BD Pharmingen, 550274, 1:200), anti-PDGFR β (eBioscience, 14-1402-82, 1:200 and Cell Signaling, 3169S, 1:200), anti-CD13 (BD Pharmingen, 558744, 1:200), anti-Cre recombinase (Novagen, 69050, 1:2000), or anti-Ki67 (Millipore, AB9260, 1:1000) antibodies overnight at 4°C, followed by fluorescent secondary antibodies (Invitrogen) for 1 hour at room temperature. FITC-conjugated SMA (Sigma, F3777, 1:1000) was used to study pericyte differentiation and distinguish capillaries and large vessels, given that SMA is expressed in arterioles and arteries but not capillaries under normal conditions. After mounting, the brain sections were examined and photographed with an Axiovert 200 (Zeiss) microscopy or Leica confocal microscopy. For quantification, at least 9 random images (from at least 3 animals) with GFP or Cre signal at 200X magnification were taken and the mean fluorescence intensity was analyzed.

TUNEL Assay

Cell death was examined using the *In Situ* Cell Death Detection Kit, TMR red (Roche), according to the manufacturer's protocol. Briefly, brain sections were fixed in 4% paraformaldehyde and permeabilized on ice, followed by incubation with TUNEL reaction mixture. After washing, the sections were examined by fluorescence microscopy.

Electron Microscopy Analysis

Two-month-old mice (both genders) were anesthetized and perfused with PBS following by 0.1M sodium cacodylate buffer containing 2% paraformaldehyde and 2% glutaraldehyde. After perfusion, the striatum was dissected out and fixed overnight. The tissue was post-fixed in 1% osmium tetroxide and 1% K-ferrocyanide. Next, the tissue was en bloc stained with 2% uranyl acetate and embedded in resin. Ultra-thin sections were cut on a Reichert-Jung Ultracut E microtome and post-stained with 2% uranyl acetate and 1% lead citrate. Sections were examined and photographed using JEOL100CXII at 80 KV.

Statistics

Results are shown as mean \pm S.D. Student's t-test, performed by SPSS Statistics or Microsoft Excel, was used to analyze differences between two groups.

Supplementary Material

Refer to Web version on PubMed Central for supplementary material.

Acknowledgments

We thank Dr. Arturo Alvarez-Buylla for adenoviruses expressing Cre under GFAP promoter (Ad-pGFAP-Cre), Dr. Jonathan Jones for the laminin α 4 blocking antibody, Lee Cohen-Gould (Weill Cornell Medical School) and Dr. Kunihiro Uryu (The Rockefeller University) for technical support and assistance with electron microscopy. We also thank Strickland lab members for scientific support and suggestions. This work was supported by NIH grant NS050537 to S.S., and Merck Postdoctoral Fellowship and BD Stem Cell Grant to Y.Y.. The funders had no role in study design, data collection and analysis, decision to publish, or preparation of the manuscript.

References

1. Persidsky Y, Ramirez SH, Haorah J, Kanmogne GD. Blood-brain barrier: structural components and function under physiologic and pathologic conditions. *J Neuroimmune Pharmacol.* 2006; 1:223–236. [PubMed: 18040800]
2. Zipser BD, et al. Microvascular injury and blood-brain barrier leakage in Alzheimer's disease. *Neurobiol Aging.* 2007; 28:977–986. [PubMed: 16782234]
3. van Vliet EA, et al. Blood-brain barrier leakage may lead to progression of temporal lobe epilepsy. *Brain.* 2007; 130:521–534. [PubMed: 17124188]
4. Wardlaw JM, et al. Lacunar stroke is associated with diffuse blood-brain barrier dysfunction. *Ann Neurol.* 2009; 65:194–202. [PubMed: 19260033]
5. Guillemin GJ, Brew BJ. Microglia, macrophages, perivascular macrophages, and pericytes: a review of function and identification. *J Leukoc Biol.* 2004; 75:388–397. [PubMed: 14612429]
6. Romero IA, et al. Changes in cytoskeletal and tight junctional proteins correlate with decreased permeability induced by dexamethasone in cultured rat brain endothelial cells. *Neurosci Lett.* 2003; 344:112–116. [PubMed: 12782340]
7. Wolburg H, Lippoldt A. Tight junctions of the blood-brain barrier: development, composition and regulation. *Vascul Pharmacol.* 2002; 38:323–337. [PubMed: 12529927]
8. Daneman R, Zhou L, Kebede AA, Barres BA. Pericytes are required for blood-brain barrier integrity during embryogenesis. *Nature.* 2010
9. Armulik A, et al. Pericytes regulate the blood-brain barrier. *Nature.* 2010; 468:557–561. [PubMed: 20944627]
10. Bell RD, et al. Pericytes control key neurovascular functions and neuronal phenotype in the adult brain and during brain aging. *Neuron.* 2010; 68:409–427. [PubMed: 21040844]

11. Kwon I, Kim EH, del Zoppo GJ, Heo JH. Ultrastructural and temporal changes of the microvascular basement membrane and astrocyte interface following focal cerebral ischemia. *J Neurosci Res.* 2009; 87:668–676. [PubMed: 18831008]
12. Wang CX, Shuaib A. Critical role of microvasculature basal lamina in ischemic brain injury. *Prog Neurobiol.* 2007; 83:140–148. [PubMed: 17868971]
13. Cardoso FL, Brites D, Brito MA. Looking at the blood-brain barrier: molecular anatomy and possible investigation approaches. *Brain Res Rev.* 2010; 64:328–363. [PubMed: 20685221]
14. Balabanov R, Dore-Duffy P. Role of the CNS microvascular pericyte in the blood-brain barrier. *J Neurosci Res.* 1998; 53:637–644. [PubMed: 9753191]
15. Fisher M. Pericyte signaling in the neurovascular unit. *Stroke.* 2009; 40:S13–15. [PubMed: 19064799]
16. Shepro D, Morel NM. Pericyte physiology. *FASEB J.* 1993; 7:1031–1038. [PubMed: 8370472]
17. Sorokin LM, et al. Developmental regulation of the laminin alpha5 chain suggests a role in epithelial and endothelial cell maturation. *Dev Biol.* 1997; 189:285–300. [PubMed: 9299121]
18. Sixt M, et al. Endothelial cell laminin isoforms, laminins 8 and 10, play decisive roles in T cell recruitment across the blood-brain barrier in experimental autoimmune encephalomyelitis. *J Cell Biol.* 2001; 153:933–946. [PubMed: 11381080]
19. Jucker M, Tian M, Norton DD, Sherman C, Kusiak JW. Laminin alpha 2 is a component of brain capillary basement membrane: reduced expression in dystrophic dy mice. *Neuroscience.* 1996; 71:1153–1161. [PubMed: 8684619]
20. Stratman AN, Malotte KM, Mahan RD, Davis MJ, Davis GE. Pericyte recruitment during vasculogenic tube assembly stimulates endothelial basement membrane matrix formation. *Blood.* 2009; 114:5091–5101. [PubMed: 19822899]
21. Chen ZL, et al. Ablation of astrocytic laminin impairs vascular smooth muscle cell function and leads to hemorrhagic stroke. *J Cell Biol.* 2013; 202:381–395. [PubMed: 23857767]
22. Dore-Duffy P, Katychew A, Wang X, Van Buren E. CNS microvascular pericytes exhibit multipotential stem cell activity. *J Cereb Blood Flow Metab.* 2006; 26:613–624. [PubMed: 16421511]
23. Yu WM, Feltri ML, Wrabetz L, Strickland S, Chen ZL. Schwann cell-specific ablation of laminin gamma1 causes apoptosis and prevents proliferation. *J Neurosci.* 2005; 25:4463–4472. [PubMed: 15872093]
24. Chen ZL, Haegeli V, Yu H, Strickland S. Cortical deficiency of laminin gamma1 impairs the AKT/GSK-3beta signaling pathway and leads to defects in neurite outgrowth and neuronal migration. *Dev Biol.* 2009; 327:158–168. [PubMed: 19118544]
25. Bernacki J, Dobrowolska A, Nierwinska K, Malecki A. Physiology and pharmacological role of the blood-brain barrier. *Pharmacol Rep.* 2008; 60:600–622. [PubMed: 19066407]
26. Citi S, Cordenonsi M. Tight junction proteins. *Biochim Biophys Acta.* 1998; 1448:1–11. [PubMed: 9824655]
27. Huber JD, Egleton RD, Davis TP. Molecular physiology and pathophysiology of tight junctions in the blood-brain barrier. *Trends Neurosci.* 2001; 24:719–725. [PubMed: 11718877]
28. Armulik A, Genove G, Betsholtz C. Pericytes: developmental, physiological, and pathological perspectives, problems, and promises. *Dev Cell.* 2011; 21:193–215. [PubMed: 21839917]
29. Dore-Duffy P. Pericytes: pluripotent cells of the blood brain barrier. *Curr Pharm Des.* 2008; 14:1581–1593. [PubMed: 18673199]
30. Thanabalasundaram G, Schneidewind J, Pieper C, Galla HJ. The impact of pericytes on the blood-brain barrier integrity depends critically on the pericyte differentiation stage. *Int J Biochem Cell Biol.* 2011; 43:1284–1293. [PubMed: 21601005]
31. Dore-Duffy P, Cleary K. Morphology and properties of pericytes. *Methods Mol Biol.* 2011; 686:49–68. [PubMed: 21082366]
32. Liebner S, et al. Claudin-1 and claudin-5 expression and tight junction morphology are altered in blood vessels of human glioblastoma multiforme. *Acta Neuropathol.* 2000; 100:323–331. [PubMed: 10965803]

33. Dore-Duffy P, LaManna JC. Physiologic angiodynamics in the brain. *Antioxid Redox Signal*. 2007; 9:1363–1371. [PubMed: 17627476]
34. Verbeek MM, Otte-Holler I, Wesseling P, Ruiter DJ, de Waal RM. Induction of alpha-smooth muscle actin expression in cultured human brain pericytes by transforming growth factor-beta 1. *Am J Pathol*. 1994; 144:372–382. [PubMed: 8311120]
35. Sieczkiewicz GJ, Herman IM. TGF-beta 1 signaling controls retinal pericyte contractile protein expression. *Microvasc Res*. 2003; 66:190–196. [PubMed: 14609524]
36. Bonkowski D, Katyshev V, Balabanov RD, Borisov A, Dore-Duffy P. The CNS microvascular pericyte: pericyte-astrocyte crosstalk in the regulation of tissue survival. *Fluids Barriers CNS*. 2011; 8:8. [PubMed: 21349156]
37. Hultgardh-Nilsson A, Durbeek M. Role of the extracellular matrix and its receptors in smooth muscle cell function: implications in vascular development and disease. *Curr Opin Lipidol*. 2007; 18:540–545. [PubMed: 17885425]
38. Thyberg J, Hultgardh-Nilsson A. Fibronectin and the basement membrane components laminin and collagen type IV influence the phenotypic properties of subcultured rat aortic smooth muscle cells differently. *Cell Tissue Res*. 1994; 276:263–271. [PubMed: 8020062]
39. Chow N, et al. Serum response factor and myocardin mediate arterial hypercontractility and cerebral blood flow dysregulation in Alzheimer's phenotype. *Proc Natl Acad Sci U S A*. 2007; 104:823–828. [PubMed: 17215356]
40. Wang DZ, Olson EN. Control of smooth muscle development by the myocardin family of transcriptional coactivators. *Curr Opin Genet Dev*. 2004; 14:558–566. [PubMed: 15380248]
41. Hurley JV. An electron microscopic study of leucocytic emigration and vascular permeability in rat skin. *Aust J Exp Biol Med Sci*. 1963; 41:171–186. [PubMed: 13955841]
42. Nourshargh S, Hordijk PL, Sixt M. Breaching multiple barriers: leukocyte motility through venular walls and the interstitium. *Nat Rev Mol Cell Biol*. 2010; 11:366–378. [PubMed: 20414258]
43. Zlokovic BV. Neurovascular pathways to neurodegeneration in Alzheimer's disease and other disorders. *Nat Rev Neurosci*. 2011; 12:723–738. [PubMed: 22048062]
44. Erlichman JS, Leiter JC, Gourine AV. ATP, glia and central respiratory control. *Respir Physiol Neurobiol*. 2010; 173:305–311. [PubMed: 20601205]
45. Zhang Y, Barres BA. Astrocyte heterogeneity: an underappreciated topic in neurobiology. *Curr Opin Neurobiol*. 2010; 20:588–594. [PubMed: 20655735]
46. Hewett JA. Determinants of regional and local diversity within the astroglial lineage of the normal central nervous system. *J Neurochem*. 2009; 110:1717–1736. [PubMed: 19627442]
47. Nico B, et al. Severe alterations of endothelial and glial cells in the blood-brain barrier of dystrophic mdx mice. *Glia*. 2003; 42:235–251. [PubMed: 12673830]
48. Nico B, et al. Altered blood-brain barrier development in dystrophic MDX mice. *Neuroscience*. 2004; 125:921–935. [PubMed: 15120852]
49. Robel S, et al. Conditional deletion of beta1-integrin in astroglia causes partial reactive gliosis. *Glia*. 2009; 57:1630–1647. [PubMed: 19373938]
50. Diaz-Flores L, et al. Pericytes. Morphofunction, interactions and pathology in a quiescent and activated mesenchymal cell niche. *Histol Histopathol*. 2009; 24:909–969. [PubMed: 19475537]
51. Goritz C, et al. A pericyte origin of spinal cord scar tissue. *Science*. 2011; 333:238–242. [PubMed: 21737741]
52. Majesky MW, Dong XR, Regan JN, Høglund VJ. Vascular smooth muscle progenitor cells: building and repairing blood vessels. *Circ Res*. 2011; 108:365–377. [PubMed: 21293008]
53. Peppiatt CM, Howarth C, Mobbs P, Attwell D. Bidirectional control of CNS capillary diameter by pericytes. *Nature*. 2006; 443:700–704. [PubMed: 17036005]
54. Yemisci M, et al. Pericyte contraction induced by oxidative-nitrative stress impairs capillary reflow despite successful opening of an occluded cerebral artery. *Nat Med*. 2009; 15:1031–1037. [PubMed: 19718040]
55. Fernandez-Klett F, Offenhauser N, Dirnagl U, Priller J, Lindauer U. Pericytes in capillaries are contractile in vivo, but arterioles mediate functional hyperemia in the mouse brain. *Proc Natl Acad Sci U S A*. 2010; 107:22290–22295. [PubMed: 21135230]

56. Wiedeman MP. Dimensions of blood vessels from distributing artery to collecting vein. *Circ Res.* 1963; 12:375–378. [PubMed: 14000509]
57. Loulier K, et al. beta1 integrin maintains integrity of the embryonic neocortical stem cell niche. *PLoS Biol.* 2009; 7:e1000176. [PubMed: 19688041]
58. Graus-Porta D, et al. Beta1-class integrins regulate the development of laminae and folia in the cerebral and cerebellar cortex. *Neuron.* 2001; 31:367–379. [PubMed: 11516395]
59. Haubst N, Georges-Labouesse E, De Arcangelis A, Mayer U, Gotz M. Basement membrane attachment is dispensable for radial glial cell fate and for proliferation, but affects positioning of neuronal subtypes. *Development.* 2006; 133:3245–3254. [PubMed: 16873583]
60. Bell RD, et al. Apolipoprotein E controls cerebrovascular integrity via cyclophilin A. *Nature.* 2012; 485:512–516. [PubMed: 22622580]
61. Zlokovic BV, Mackic JB, Wang L, McComb JG, McDonough A. Differential expression of Na,K-ATPase alpha and beta subunit isoforms at the blood-brain barrier and the choroid plexus. *J Biol Chem.* 1993; 268:8019–8025. [PubMed: 8385133]
62. Bake S, Friedman JA, Sohrabji F. Reproductive age-related changes in the blood brain barrier: expression of IgG and tight junction proteins. *Microvasc Res.* 2009; 78:413–424. [PubMed: 19591848]

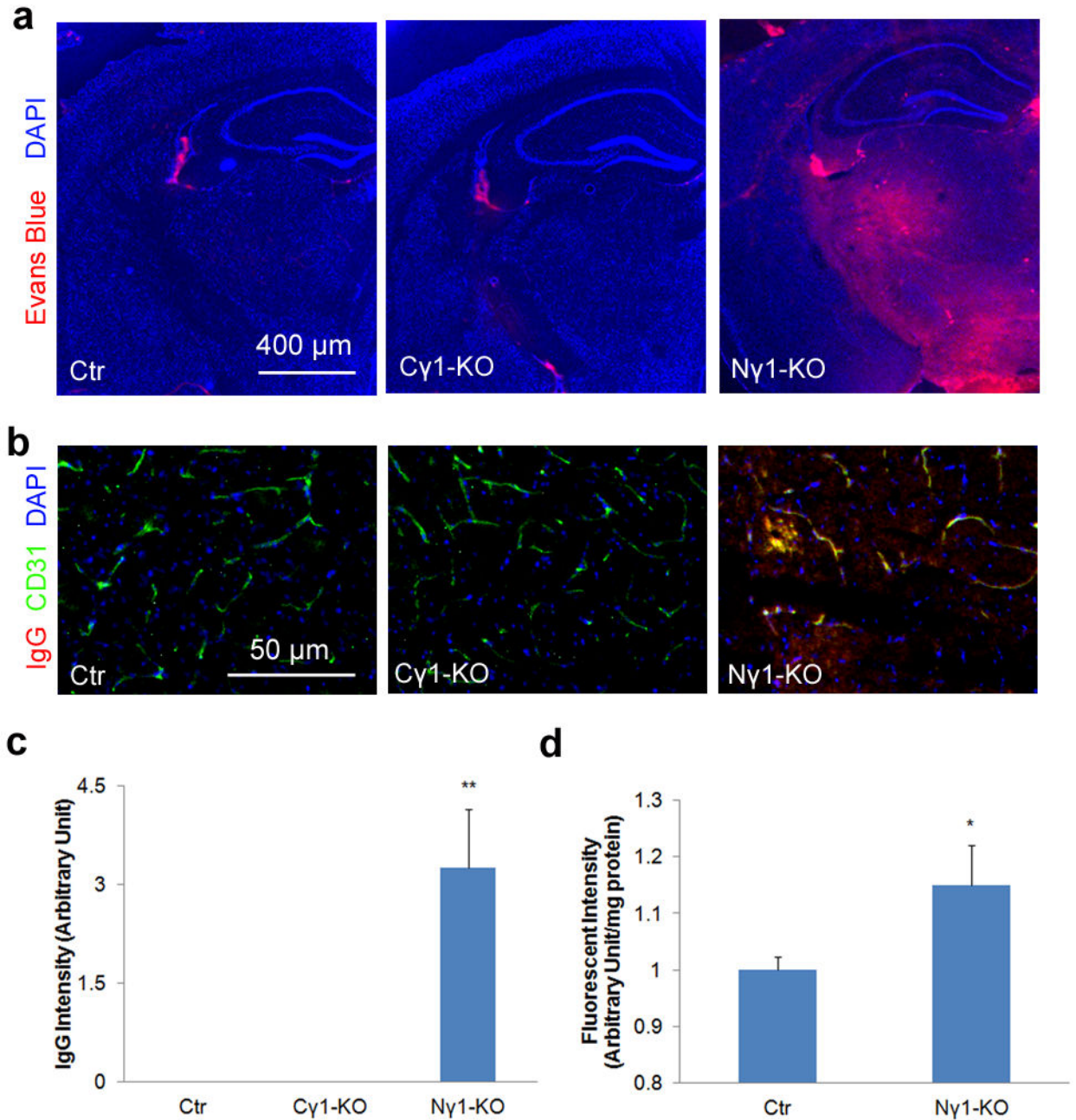


Figure 1.

BBB integrity is compromised in N γ 1-KO mice. Mice were injected with Evans blue intraperitoneally 12 hours before the mice were sacrificed. After perfusion, brain sections were used to examine Evans blue directly under fluorescent microscopy and mouse IgG by immunohistochemistry. (**a** and **b**) Evans blue (**a**) and mouse IgG (**b**) infiltrate the brain parenchyma of N γ 1-KO but not Ctr or C γ 1-KO mice. (**c**) Quantification of mouse IgG intensity in the brain parenchyma of N γ 1-KO mice. Data are quantified using 9 sections from 3 animals. (**d**) Quantification of FITC-Dextran in the brain parenchyma. FITC-Dextran (500 kDa) was injected intravenously 12 hours before mice were sacrificed. After perfusion,

brains were collected and homogenized. Infiltrated FITC-Dextran was quantified using a fluorescence plate reader at 485 nm (n=3). Scale bars represent 400 μm (**a**) and 50 μm (**b**). Data are shown as mean \pm sd. *p<0.05 and **p<0.001 versus the Ctrs by student's t-test.

Author Manuscript

Author Manuscript

Author Manuscript

Author Manuscript

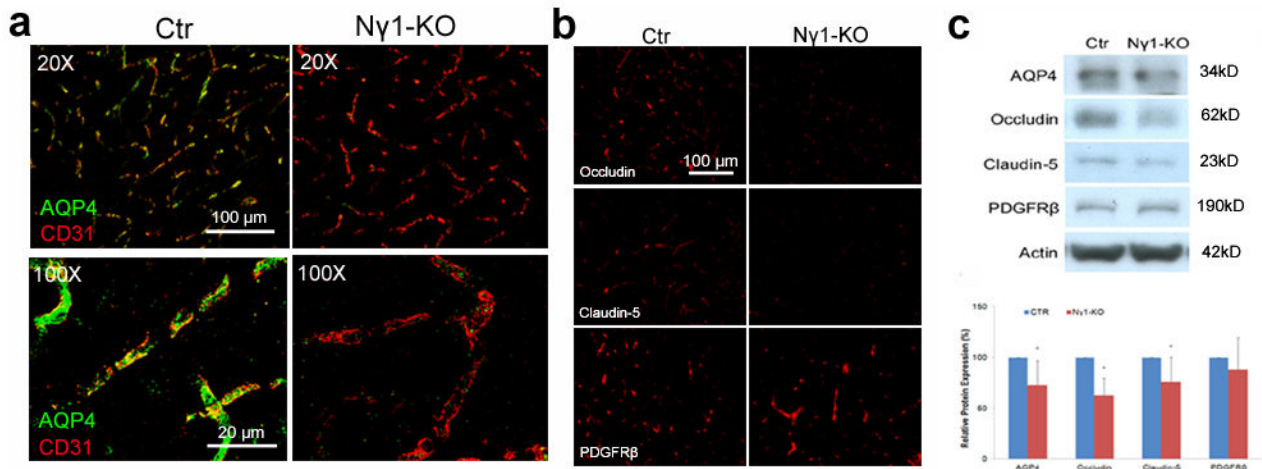


Figure 2.

Individual BBB components are affected in the N γ 1-KO brains. **(a)** Immunohistochemistry shows that astrocytic endfeet marker AQP4 is expressed at high level in Ctr mice, but dramatically reduced in N γ 1-KO mice. High power confocal Z-projection images show that AQP4 co-localizes with endothelial cell marker CD31 in Ctr but not N γ 1-KO brains. **(b)** Occludin and claudin-5, but not PDGFR β , are significantly decreased in N γ 1-KO brains. **(c)** Representative Western blot of AQP4, occludin, claudin-5, PDGFR β , and actin using striatum lysates from Ctr and N γ 1-KO mice. Full blots of these proteins are shown in Supplementary Figure 14a. Western blot was quantified by densitometry. All bands were normalized to actin (n=6). Scale bars represent 100 μ m (low magnification images in **a** and **b**) and 20 μ m (high magnification images in **a**). Data are shown as mean \pm sd. *p<0.05 versus the Ctrs by student's t-test.

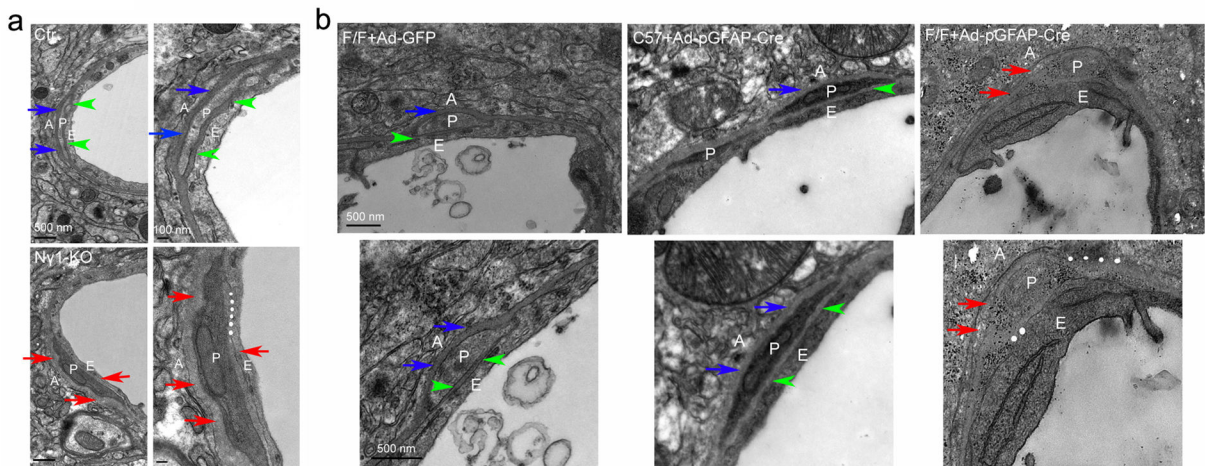
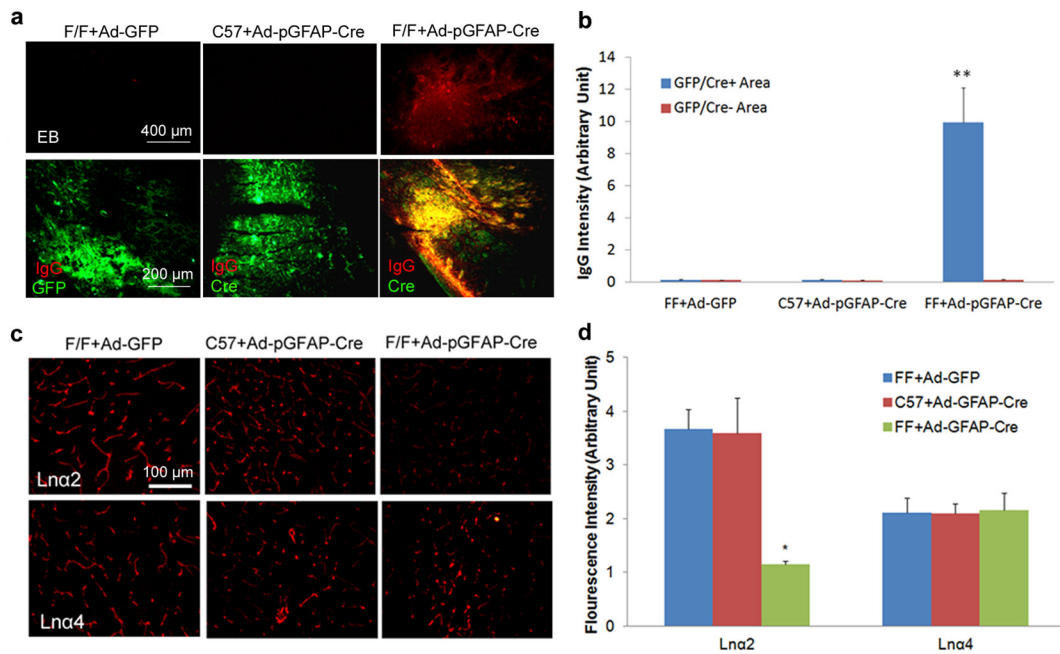


Figure 3.

Ultrastructural changes in $N\gamma 1$ -KO and laminin-knockdown brains. **(a)** In Ctr mice, the BM between astrocytes and pericytes (blue arrows) and that between pericytes and endothelial cells (green arrowheads) are compact and pericytes are tightly attached to endothelial cells. In the $N\gamma 1$ -KO mice, however, pericytes change their morphology and both BMs show a patchy and diffused pattern (red arrows). Moreover, the endothelial membrane integrity is compromised at some places (white stars) in $N\gamma 1$ -KO mice. **(b)** In Ctr mice (F/F+Ad-GFP and C57+Ad-pGFAP-Cre), pericytes are surrounded by nicely aligned and compact BMs secreted by both astrocytes (blue arrows) and endothelial cells (green arrowheads). In astrocytic laminin-knockdown mice (F/F+Ad-pGFAP-Cre), on the other hand, pericytes change their morphology and both BMs become patchy and diffuse (red arrows). In addition, the BMs are hard to define at some places and the membrane integrity is severely compromised in these astrocytic laminin-knockdown mice (white stars). A: Astrocytes; P: Pericytes; E: Endothelia. Scale bars represent 500 nm (low magnification images in **a** on the left and **b**), and 100 nm (high magnification images in **a** on the right).

**Figure 4.**

Acute ablation of astrocytic laminin leads to BBB breakdown. Mice were injected with adenovirus as indicated. Seven days after injection, the brains were collected and analyzed. **(a)** Evans blue and mouse IgG infiltrate into the brain parenchyma of F/F mice with Ad-pGFAP-Cre injection, but not the Ctr F/F mice with Ad-GFP injection or C57Bl6 mice with Ad-pGFAP-Cre injection. GFP (for Ad-GFP injected brains) and Cre (for Ad-pGFAP-Cre injected brains) were used to reveal infected regions. **(b)** Quantification of IgG intensity in GFP/Cre positive and negative areas in adenovirus-injected mouse brains. Data are quantified using 9 sections from 3 animals per group. **(c)** Laminin is specifically knocked down in astrocytes by adenoviruses. Seven days after adenoviral injection, brains were collected and immunostained for laminin $\alpha 2$ (Lna2, marker for astrocytic laminin) and $\alpha 4$ (Lna4, marker for endothelial laminin). Our data show that the adenoviruses we used specifically knocked down astrocytic laminin without affecting endothelial laminin. **(d)** Quantification of Lna2 and Lna4 intensity in the brain parenchyma of the adenovirus-injected mice. Data are quantified using 6 sections from 3 animals per group. Scale bars represent 400 μm (EB in **a**), 200 μm (IgG in **a**) and 100 μm (**c**). Data are shown as mean \pm sd. * $p < 0.05$ and ** $p < 0.001$ versus the Ctr by student's t-test.

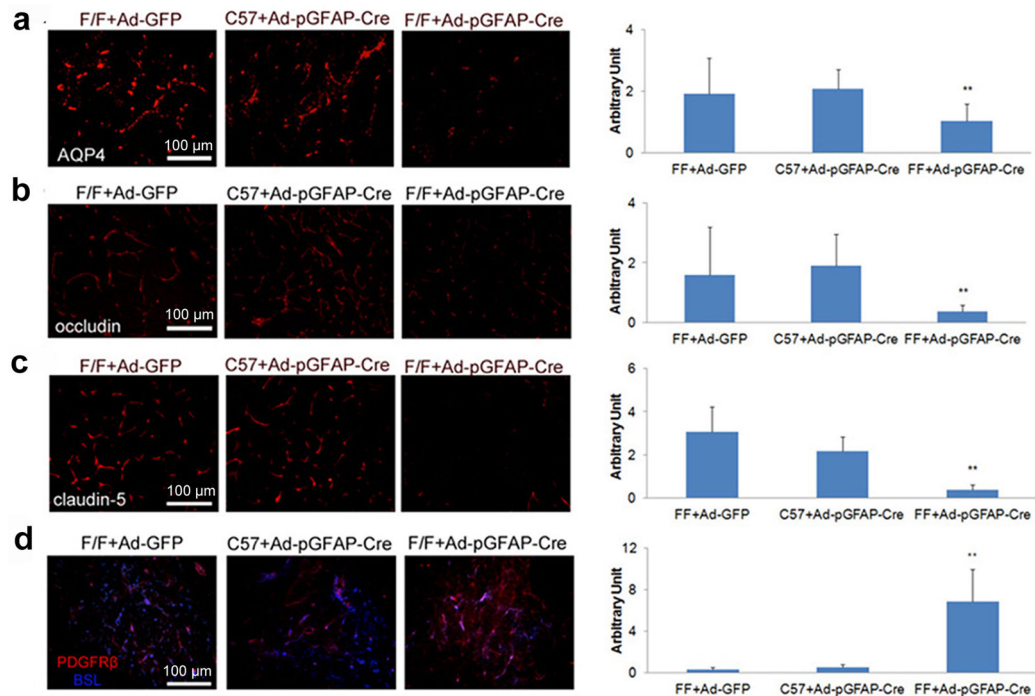


Figure 5.

Acute ablation of astrocytic laminin affects individual BBB components. Mice were injected with adenovirus as indicated. Seven days after injection, the brains were collected and analyzed. **(a)** Immunohistochemistry shows that astrocytic endfeet marker AQP4 is significantly decreased in F/F mice with Ad-pGFAP-Cre injection, but not in the Ctrs--- F/F mice with Ad-GFP injection or C57 mice with Ad-pGFAP-Cre injection. AQP4 fluorescence intensity was quantified using 12–13 random sections from 3 or more mice per group. **(b)** and **(c)** Immunohistochemistry shows that occludin **(b)** and claudin-5 **(c)** are significantly decreased in F/F mice with Ad-pGFAP-Cre injection, but not in the Ctrs. The fluorescence intensity of these proteins was quantified using 9–13 random sections from at least 3 mice per group. **(d)** Immunohistochemistry shows that the pericyte marker PDGFR β is significantly increased in F/F mice with Ad-pGFAP-Cre injection, but not in the Ctrs. PDGFR β fluorescence intensity was quantified using 11–12 random sections from at least 3 mice per group. Scale bars represent 100 μ m. Data are shown as mean \pm sd. ** $p < 0.001$ versus the Ctrs by student's t-test.

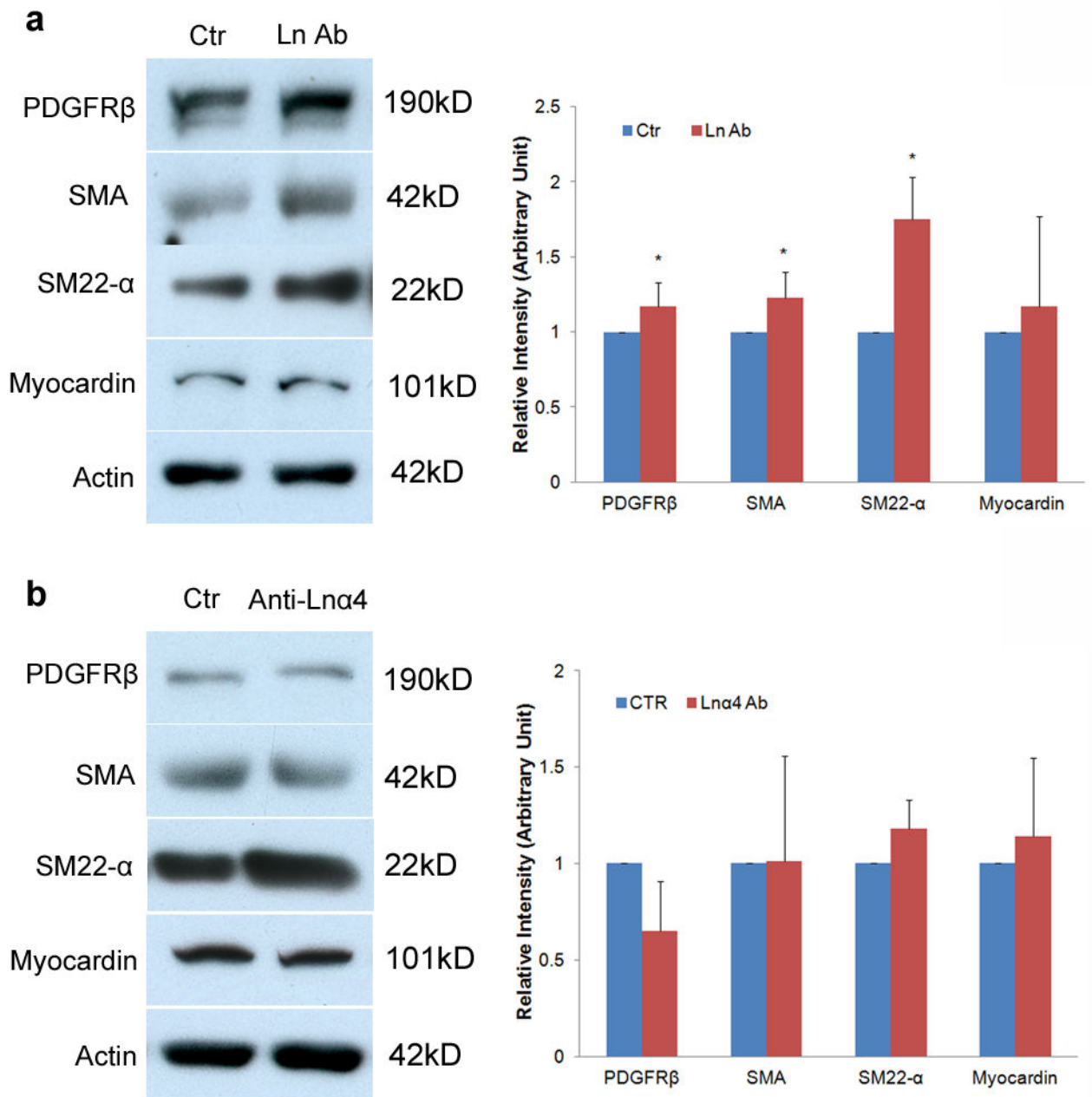
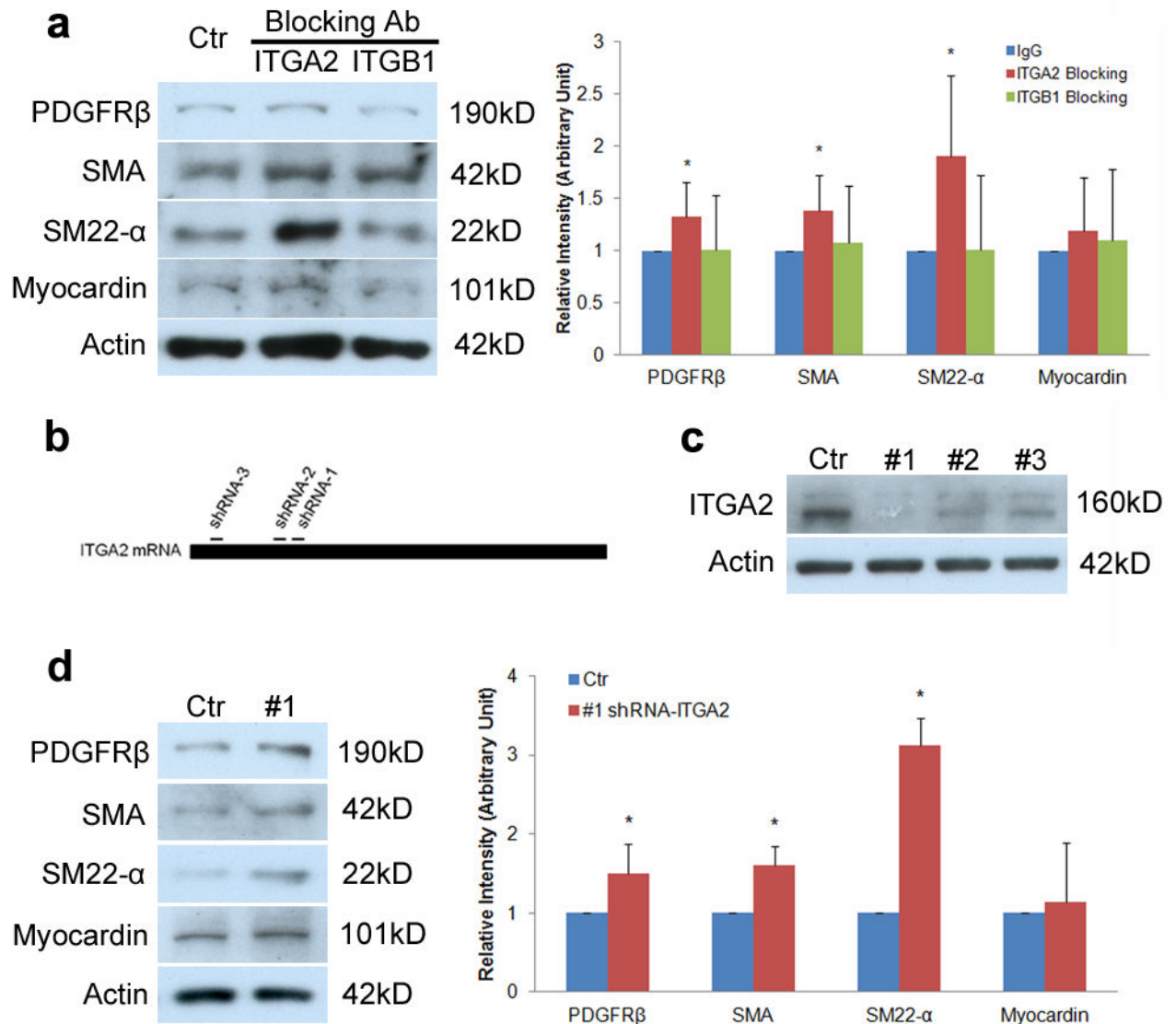


Figure 6. Laminin-111 but not laminin- α 4 blocking antibody affects pericyte differentiation. **(a)** Immunoblots show that laminin-111 blockage (Ln Ab) significantly enhances the expression of PDGFR β , SMA, and SM22- α , but not myocardin in pericytes. Full blots of these proteins are shown in Supplementary Figure 14b. Rabbit IgG treated cells were used as a Ctr. All bands were normalized to actin (n=5–6). **(b)** Immunoblots show that laminin- α 4 blockage (Anti-Ln α 4) does not change the expression of PDGFR β , SMA, SM22- α , or myocardin in pericytes. Full blots of these proteins are shown in Supplementary Figure 14c. Rabbit IgG treated cells were used as a Ctr. All bands were normalized to actin (n=3). Data are shown as mean \pm sd. *p<0.05 versus the Ctrs by student's t-test.

**Figure 7.**

Astrocytic laminin mediates pericyte differentiation via integrin α 2. **(a)** Immunoblots show that integrin α 2 blockage (ITGA2) but not integrin β 1 blockage significantly increases the expression of PDGFR β , SMA, and SM22- α , but not myocardin in pericytes. Full blots of these proteins are shown in Supplementary Figure 14d. Rabbit IgG treated cells were used as a Ctr. All bands were normalized to actin (n=6). **(b)** Schematic diagram of shRNA designed to target ITGA2 mRNA. **(c)** Immunoblot analysis shows that all three ITGA2-specific shRNAs (#1–3) dramatically reduce ITGA2 at protein level and ITGA2-specific shRNA-3 (#1) is the most efficient one. Full blots of ITGA2 and actin are shown in Supplementary Figure 14e. Scramble shRNA was used as a Ctr. **(d)** Immunoblot analysis shows that transduction of pericytes with lenti-shRNA-1 (#1) significantly enhances the expression of PDGFR β , SMA, and SM22- α , but does not affect myocardin level. Full blots of these proteins are shown in Supplementary Figure 14f. Scramble shRNA was used as a

Ctrl. All bands were normalized to actin (n=4-5). Data are shown as mean \pm sd. *p<0.05 versus the Ctrl by student's t-test.

Author Manuscript

Author Manuscript

Author Manuscript

Author Manuscript

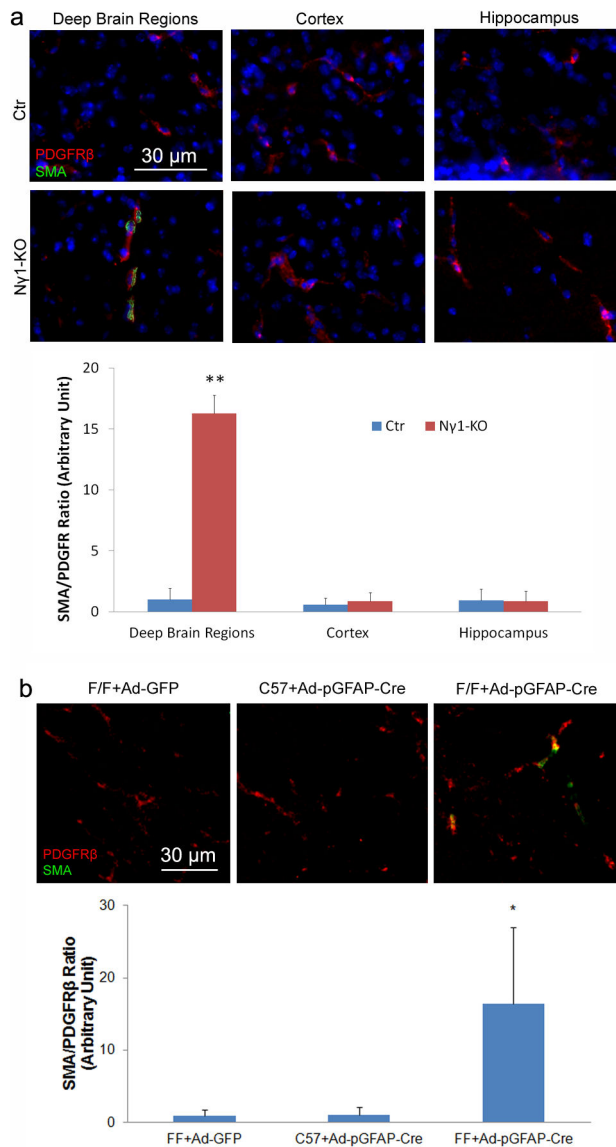
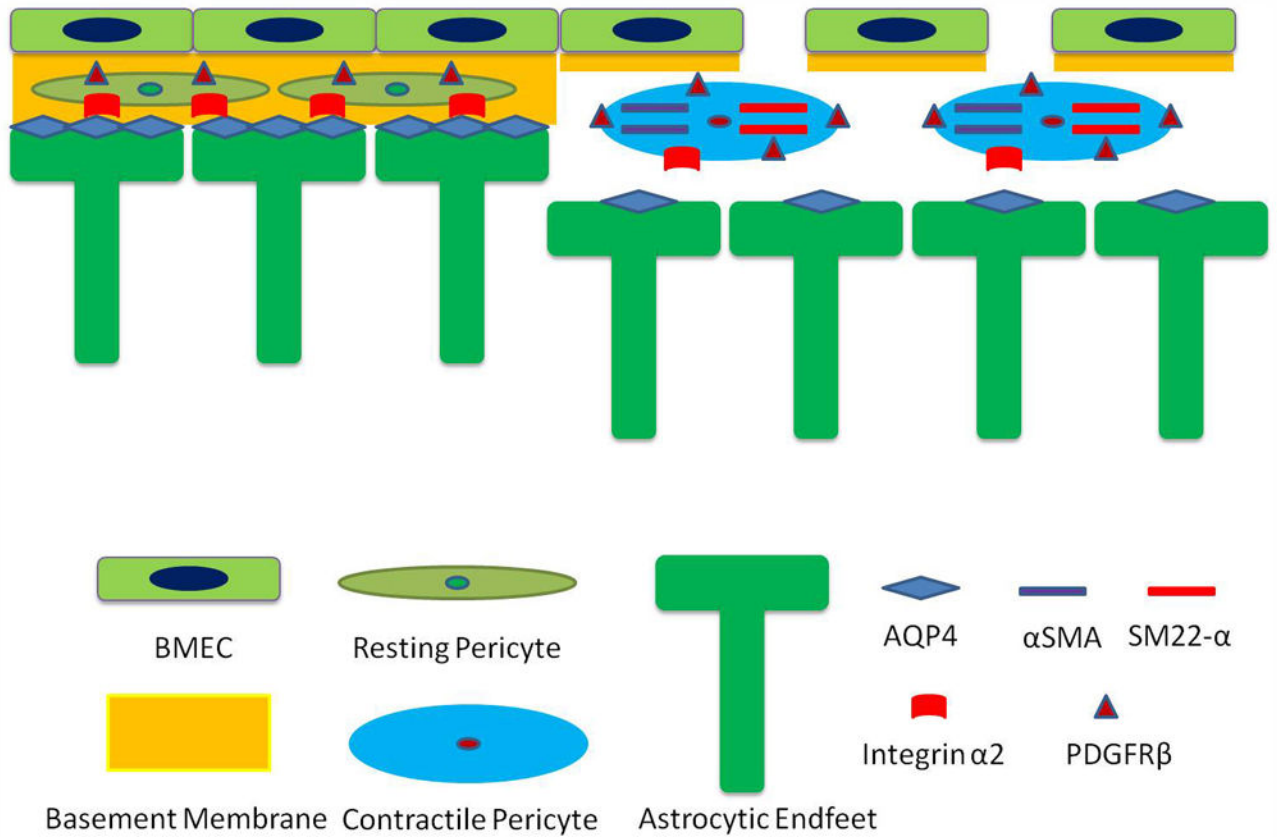


Figure 8.

Loss of astrocytic laminin increases the expression of SMA by capillary pericytes *in vivo*. Immunohistochemistry analysis shows significant enhanced SMA expression in PDGFR β positive capillary pericytes in deep brain regions of N γ 1-KO mice (**a**). In the Ctr brain or the cortex and hippocampus of N γ 1-KO mice, however, no SMA positive capillary pericytes are observed (**a**). In addition, acute ablation of astrocytic laminin by intracranial injection of adenoviruses significantly elevates the expression of SMA in PDGFR β positive pericytes (**b**). The quantification was performed by calculating the ratio of SMA intensity to PDGFR β intensity in 9–10 random sections from at least 3 mice per group. Scale bars represent 30 μ m. Data are shown as mean \pm sd. * p <0.05 and ** p <0.01 versus Ctrs by student's t-test.

**Figure 9.**

Proposed model of how astrocytic laminin affects pericyte differentiation and BBB integrity. Under physiological conditions, pericytes are embedded in the BMs produced by both astrocytes and endothelial cells. They are in the resting stage, signified by the low expression levels of PDGFR β and contractile proteins (SMA and SM-22 α). When astrocytic laminin is lost during pathological conditions, pericytes hypertrophy and the expression levels of PDGFR β and contractile proteins are enhanced, switching pericytes to their contractile stage. This process is mediated by integrin α 2. This transition changes the function of pericytes from BBB stabilization to BBB disruption. In addition, lack of astrocytic laminin also leads to reduction of AQP4 expression at astrocytic endfeet. Together these effects result in decreased expression of tight junction proteins on endothelial cells, leading to BBB breakdown and subsequent damage.